Supplement of Hydrol. Earth Syst. Sci., 27, 627–645, 2023
https://doi.org/10.5194/hess-27-627-2023-supplement

Hydrology and Earth System Sciences
Open Access

Supplement of

Climate sensitivity of the summer runoff of two glacierised Himalayan catchments with contrasting climate

Sourav Laha et al.

Correspondence to: Argha Banerjee (argha@iiserpune.ac.in)

Table S1. Details of the hydrometeorological observations used in this study. All hydro-meteorological data of upper Dudhkoshi catchment (Chevallier et al., 2017) are accessible from http://www.papredata.org/.

Parameters (station name)	Sensor	Accuracy (Range)	Data availability
Chandra catchment (Singh et al., 2020; Oulkar et al., 2022)			
Runoff (Tandi)	YSI radar	$\pm$ 2 mm	26Th June, 2016 to 30th Oct, 2018 (with gaps)
Precipitation (Himansh)	OTT Pluvio precipitation bucket	$\pm$ 0.05 mm	18th Oct, 2015 to 5th Oct, 2018 (with gaps)
2m air temperature (Himansh)	Campbell HC2S3	$\pm$0.1°C (-50 to + 60 $^{\circ}$C)	18th Oct, 2015 to 5th Oct, 2018 (with gaps)
Incoming shortwave radiation (Himansh)	Kipp and Zonen four component net radiometer	$<$ 5%–day total (305–2800 nm, 0–2000 Wm^{-2})	18th Oct, 2015 to 5th Oct, 2018 (with gaps)
Upper Dudhkoshi catchment (Chevallier et al., 2017; Sherpa et al., 2017)			
Runoff (Phadking)	Campbell sensor (details not available)		7th April 2010 to 16th April 2017
Precipitation (Phadking)	Campbell sensor (details not available)		7th April 2010 to 23th April 2017 (with gaps)
2m air temperature (Phadking)	Campbell sensor (details not available)		7th April 2010 to 23th April 2017 (with gaps)
2m air temperature (Changri Nup)	Vaisala HMP45C	$\pm$0.2°C	1st Nov, 2010 to 30th Nov, 2014
Incoming shortwave radiation (Changri Nup)	Kipp and Zonen CNR4	$\pm$3%–day total (0.305–2.8 μm)	1st Nov, 2010 to 30th Nov, 2014

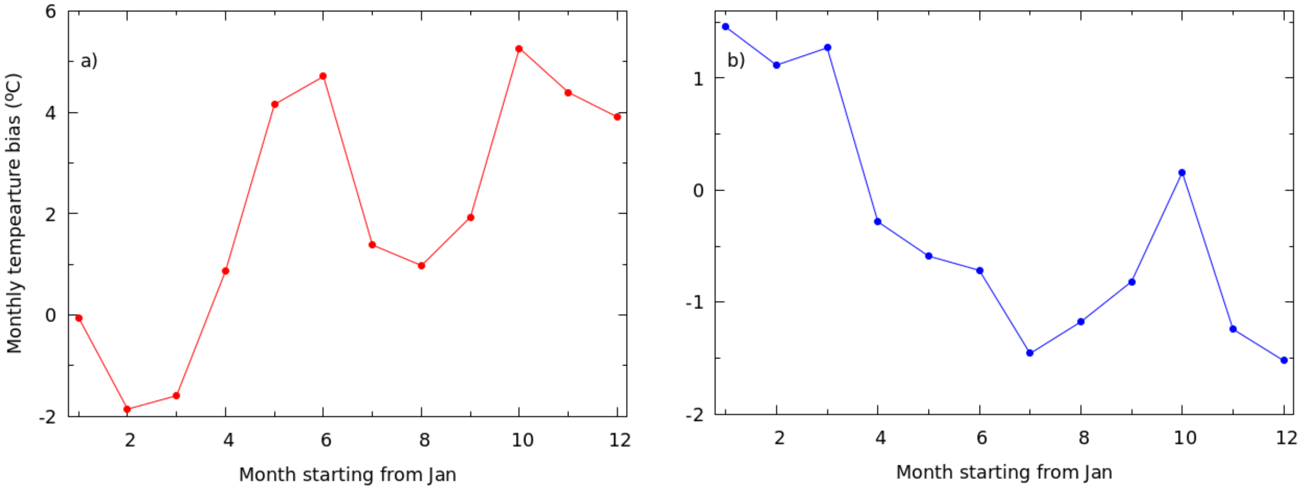

Figure S1. Mean monthly bias in ERA5 2m air temperature for (a) Chandra, and (b) upper Dudhkoshi catchments with respect to the corresponding stations (Himansh and Phadking, respectively). Here, we only considered months where the observed data gaps were less than one week. Each point in the plots represents the mean over at least 2 (5) years in Chandra (upper Dudhkoshi) catchment.

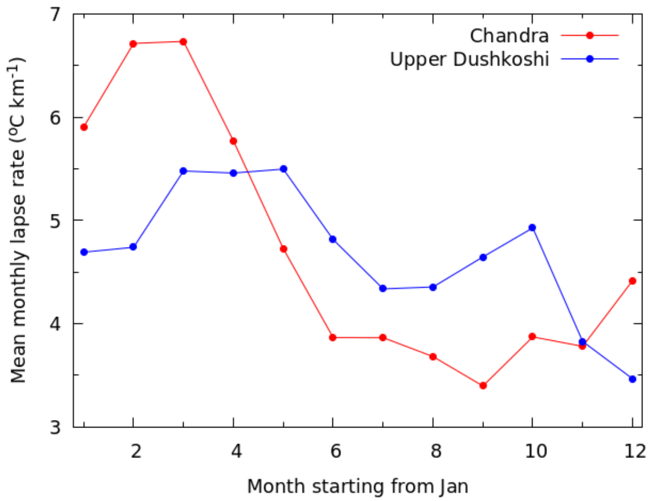

Figure S2. The mean monthly temperature lapse rates for Chandra (red symbols + line) and upper Dudhkoshi (blue symbols + line) catchments. Here, we only considered months where the observed data gaps were less than one week. Each point in the plots represents the mean over at least 2 (5) years in Chandra (upper Dudhkoshi) catchment.

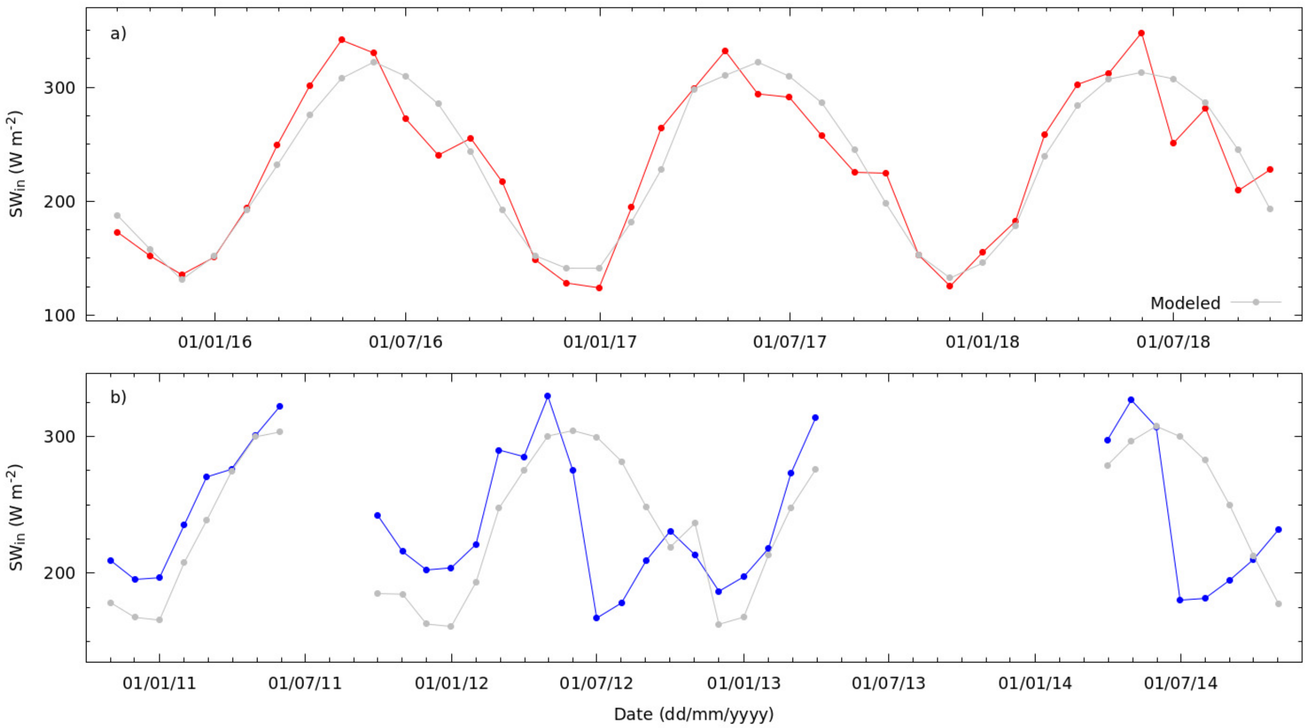

Figure S3. The incoming shortwave radiation (SW_{in}) estimated by VIC model was scaled so that it matched that observed at Himansh (Chandra catchment) and Changri Nup (upper Dudhkoshi catchment). In this plot, monthly modelled SW_{in} (gray lines + symbols) were shown for (a) Chandra, and (b) upper Dudhkoshi catchment, respectively. The corresponding monthly observed SW_{in} for Chandra (upper Dudhkoshi) catchment was shown by red lines + symbols (blue lines + symbols). In Chandra (upper Dudhkoshi) catchment the correction factor used was 2.1 (0.71).

Table S2. The values of the model parameters used in simulations. For the computation of the model errors (Sect. 3.2.3 in the main text), all the 13 model parameters were perturbed from their corresponding central values to $\pm 25\%$ of the corresponding range. While perturbing a particular or a pair of model parameters, the other parameters were kept at their central values of their corresponding ranges. Using the above procedure, we had 26 model runs for individual parameter perturbations and 78 model runs for pair wise perturbations. In total we had an ensemble of 104 model runs used for model error computation.

Parameter	Description	Range	Value used here
VIC model parameters (https://vic.readthedocs.io/en/master/)			
Ds_{max} (mm day^{-1})	Maximum velocity of baseflow	10–20	15
Ds	Fraction of Ds_{max} where nonlinear baseflow begins	0.1–0.5	0.35
Ws	Fraction of maximum soil moisture where nonlinear baseflow occurs	0.4–1.0	0.7
b_{inf}	Variable infiltration curve parameter	0.001–0.100	0.050
T_{th} (°C)	Threshold temperature for rain-snow partitioning	-1.0–1.0	0.0
α_P	Precipitation scale factor	0.7–2.5	Calibrated
Glacier runoff (Hannah and Gurnell, 2001)			
DDF (mm °C^{-1} day^{-1})	Degree day factor for ice melt	2–16	Calibrated
K_{fast} (hr)	Storage constant for fast reservoir	1–24	12
K_{slow} (hr)	Storage constant for slow reservoir	500–2000	1200
Routing model (Lohmann et al., 1998)			
UH^F_{max} (hr)	Unit hydrograph for fast flow	0.5–4.0	2
UH^F_{pow}	Parameter for shape of fast flow unit hydrograph	2–6	4
Bf (hr)	Storage constant for slow flow	1000–3000	2000
Ks (hr)	Storage constant for fast flow	100–1000	550

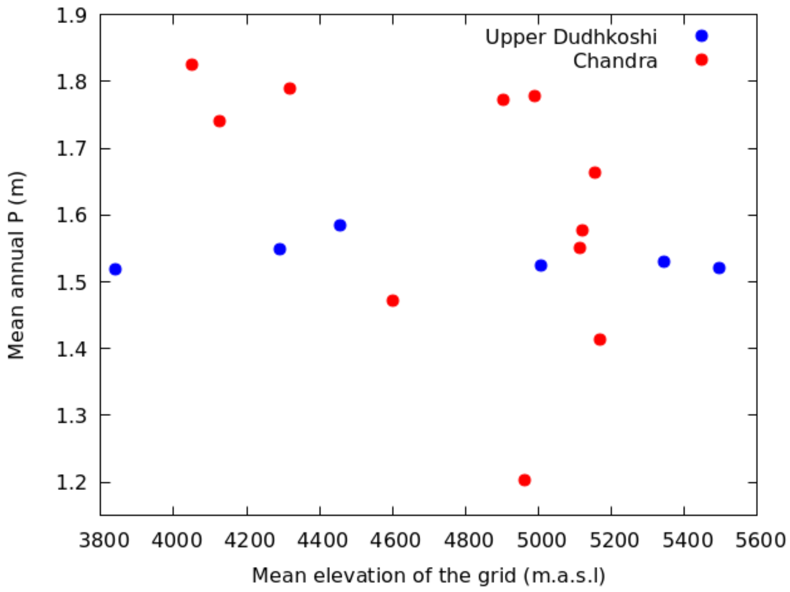

Figure S4. In Chandra and upper Dudhkoshi catchments, the mean annual precipitation of individual gridboxes are plotted against mean elevation of the corresponding gridbox.

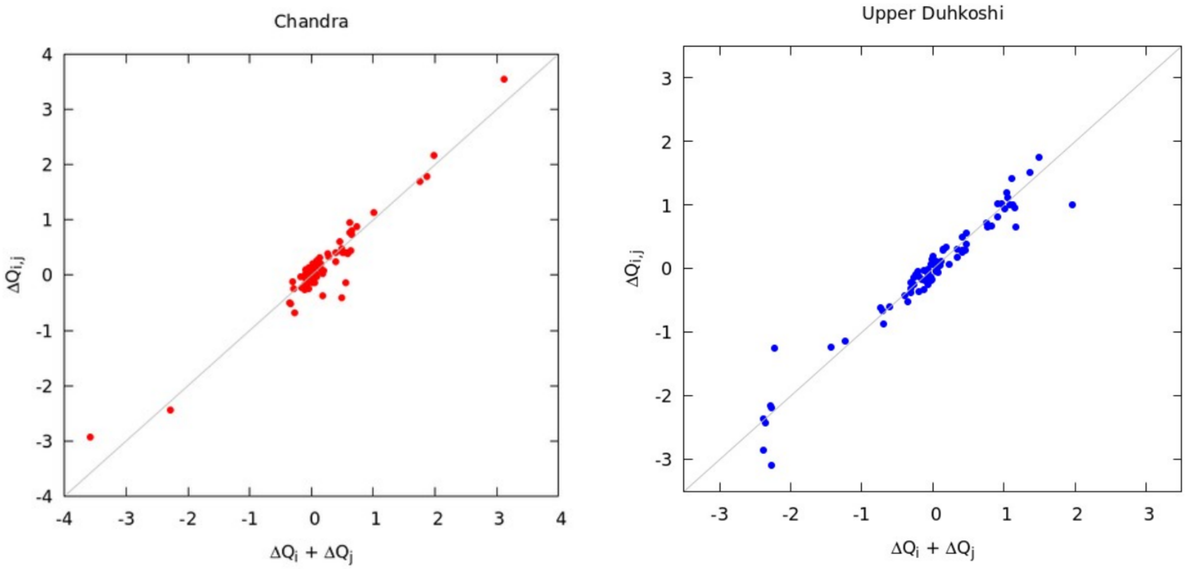

Figure S5. Percentage changes in runoff ($\Delta Q_{i,j}$) in 78 model runs, where two randomly chosen parameters out of the 13 model parameters were perturbed simultaneously, are plotted against the sum of the runoff changes ($\Delta Q_i + \Delta Q_j$) from two corresponding experiments where only one of the two parameters were perturbed.

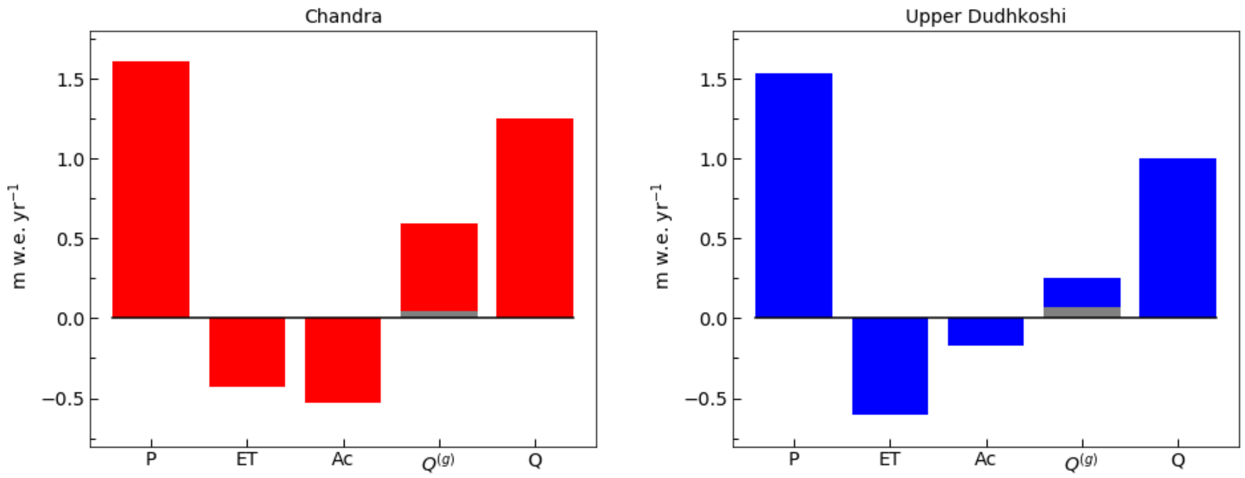

Figure S6. The components of annual hydrological balance equation $P - ET - Ac + Q^{(g)} = Q$ are shown for the two catchments. All the components are normalised by the total catchment area. P, ET, Ac, $Q^{(g)}$, and Q are the annual precipitation, evapotranspiration, glacier accumulation, the runoff from glacerised area, specific runoff from whole catchments, respectively. The imbalance contributions of the glaciers are also shown with grey bars.

Table S3. A comparison of modelled glacier mass balance with the available regional geodetic mass balance for both the catchments. For the modelled mass balance values marked with *, the modelled mean were computed starting from the year 1980. The observed geodetic mass balance values marked with † refers to corresponding catchment values, and the remaining regional values correspond to Lahul-Spiti (for Chandra catchment) and Everest/Khumbu (for upper Dudhkoshi catchment) regions.

Period	Mean modelled mass balance (m w.e yr^{-1})	Geodetic mass balance (reference) (m w.e yr^{-1})
	Chandra catchment	
1980–2018	-0.18 ± 0.10	
1980–1992	0.29 ± 0.18	
1993–2018	-0.42 ± 0.14	
1975–2000	$-0.05\pm0.11^*$	-0.13 ± 0.14 (Maurer et al., 2019)
2001–2016	-0.32 ± 0.12	-0.48 ± 0.15 (Maurer et al., 2019)
2000–2012	-0.40 ± 0.19	-0.52 ± 0.32 (Vijay and Braun, 2016)
2000–2015	-0.41 ± 0.16	-0.30 ± 0.10 (Mukherjee et al., 2018)
2000–2016	-0.41 ± 0.16	$-0.37\pm0.09^\dagger$ (Brun et al., 2017)
		$-0.31\pm0.08^\dagger$ (Shean et al., 2020)
1999–2011	-0.49 ± 0.20	-0.45 ± 0.13 (Gardelle et al., 2012)
		-0.44 ± 0.09 (Vincent et al., 2013)
	Upper Dudhkoshi catchment	
1980–2018	-0.37 ± 0.04	
1980–1992	-0.19 ± 0.07	
1993–2018	-0.46 ± 0.05	
1975–2000	$-0.29\pm0.06^*$	-0.29 ± 0.05 (Maurer et al., 2019)
1970–2007	$-0.31\pm0.05^*$	-0.31 ± 0.08 (Bolch et al., 2011)
2001–2016	-0.44 ± 0.05	-0.39 ± 0.06 (Maurer et al., 2019)
2000–2016	-0.44 ± 0.05	$-0.33\pm0.32^\dagger$ (Brun et al., 2017)
		-0.52 ± 0.22 (King et al., 2017)
		$-0.43\pm 0.25^\dagger$ (Shean et al., 2020)
1999–2011	-0.41 ± 0.06	-0.26 ± 0.13 (Gardelle et al., 2012)
1992–2008	-0.43 ± 0.06	-0.42 ± 0.30 (Nuimura et al., 2012)

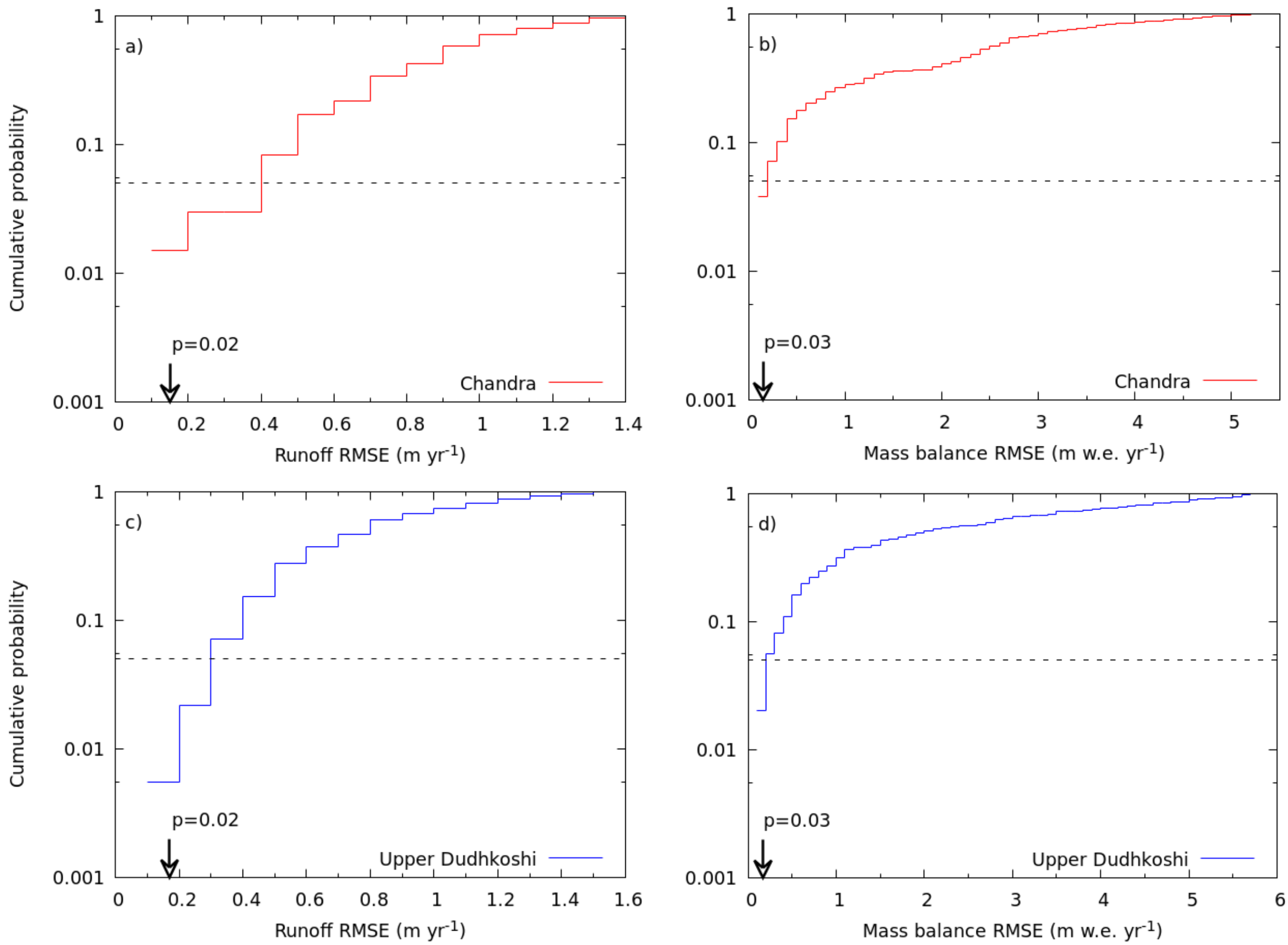

Figure S7. Cumulative probability distribution of the runoff and glacier mass balance RMSE's where a random model was chosen from the entire 319 models (Sect. 3.2.3 of the main text) for Chandra (a,b) and Upper Dudhkoshi (c,d) catchments. The horizontal dash line denotes the models with $p < 0.05$. The black arrow on the x-axis denotes the corresponding RMSE values for the best fit model.

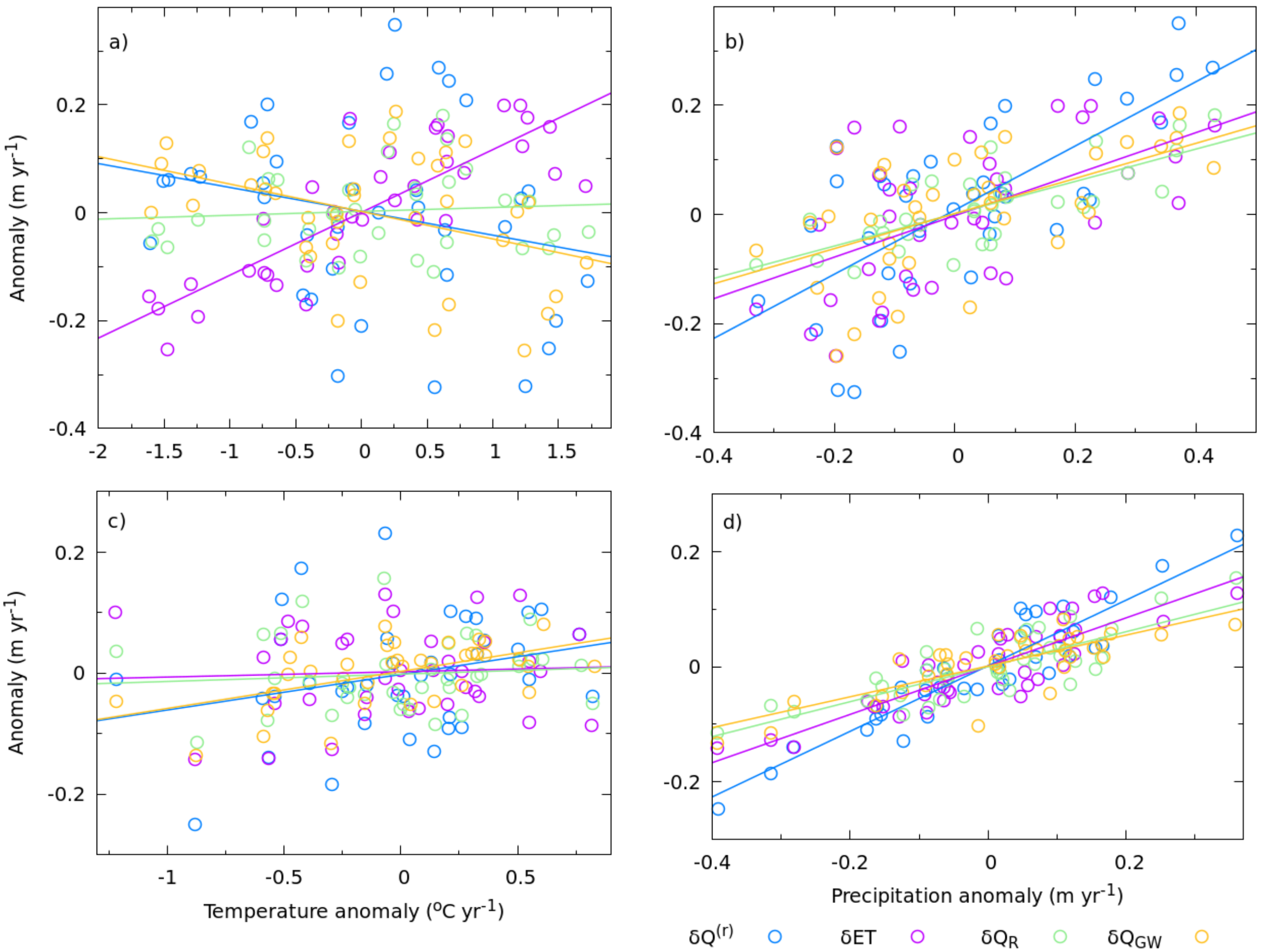

Figure S8. The anomalies of glacier off-runoff ($\delta Q^{(r)}$), and its components, surface runoff (δQ_R) and groundwater/baseflow (δQ_{GW}) are plotted here. The corresponding evapotranspiration (δET) anomalies are also shown. (a)–(b) are the plots for Chandra catchment, and (c)–(d) for upper Dudhkoshi catchment, respectively.

Table S4. A comparison between the estimated glacier ice melt contribution to annual runoff from this study and that of from the available literature.

Study area	Glacerised fraction	Reference	% of glacier ice melt contribution to annual runoff
Chandra catchment	0.25	This study	31 ± 11
Chhota Shigri glacier	0.50	Azam et al. (2019)	18 ± 3
		Engelhardt et al. (2017)	33 ± 4
Upper Dudhkoshi catchment	0.20	This study	28 ± 9
Dudhkoshi catchment	0.13	Nepal (2016)	5
		Chandel and Ghosh (2021)	8
Periche catchment	0.43	Mimeau et al. (2018)	45

Table S5. Percentage sensitivity values for both the studied catchments are given below.

Sensitivity parameter	Chandra catchment	Upper dushkoshi catchment
Catchment summer runoff sensitivities		
s_T (% of runoff per $^\circ$C warming)	11±3	14±6
s_P (% of runoff due to 10% change in P)	6±3	9±4
Glacier and off-glacier summer runoff sensitivities		
$s_T^{(g)}$ (% of runoff per $^\circ$C warming)	37±3	58±9
$s_T^{(r)}$ (% of runoff per $^\circ$C warming)	2±3	3±6
$s_P^{(g)}$ (% of runoff due to 10% change in P)	-2±3	0±2
$s_P^{(r)}$ (% of runoff due to 10% change in P)	9±3	9±4

Table S6. Comparison of our estimates of catchment runoff sensitivities with that of reported in the Himalaya and elsewhere.

Catchment name	s_T (% of runoff per °C warming)	s_P (% of runoff due to 10% change in P)	Reference
Engabreen	24	2	Engelhardt et al. (2015)
Ålfotbreen	17	6	Engelhardt et al. (2015)
Nigardsbreen	21	4	Engelhardt et al. (2015)
Storbreen	19	3.3	Engelhardt et al. (2015)
Ala-Archa	9	7	He (2021)
Dokriani	20	16	Azam and Srivastava (2020)
Dudhkoshi	5	10	Pokhrel et al. (2014)
Trambau	27	-0.6	Fujita and Sakai (2014)
Chandra	11±3	6±3	This study
Upper Dudhkoshi	14±6	9±4	This study

Table S7. Comparison of our estimates of climate sensitivity of glacier runoff with that of reported in the Himalaya and elsewhere.

Catchment name	$s_T^{(g)}$ (% of runoff per °C warming)	$s_P^{(g)}$ (% of runoff due to 10% change in P)	Reference
Midtre Lovenbreen	55	1	Pramanik et al. (2018)
Kongsvegen	71	3	Pramanik et al. (2018)
Kronebreen-Holtedahlfonna	55	4	Pramanik et al. (2018)
Brewster glacier	60	4	Anderson et al. (2010)
La Paz, Bolivia		6	Soruco et al. (2015)
Trambau	53	-7	Fujita and Sakai (2014)
Chandra	37 ± 3	-2 ± 3	This study
Upper Dudhkoshi	58 ± 9	0 ± 2	This study

Table S8. A comparison of glacier mass balance sensitivities to temperature and precipitation from this study with those available in the literature.

Catchment	References	Glacier mass balance sensitivity to	
		Temperature (m yr^{-1} °C^{-1})	Precipitation (m yr^{-1}, relative to 10% change in precipitation)
Regional values			
Chandra	This study	-0.47±0.09	0.2±0.04
Chandra	Tawde et al. (2017)	-0.16	0.09
4 western Himalayan glaciers	Wang et al. (2019)	-0.24 to -0.83	0.06 to 0.09
Indus basin	Shea and Immerzeel (2016)	-0.31 to -0.79	
Upper Dudhkoshi	This study	-0.27±0.05	0.05±0.02
Dudhkoshi	Sakai and Fujita (2017)	-0.17 to -0.36	
5 Eastern/central Himalayan glaciers	Wang et al. (2019)	-0.56 to -1.00	0.05 to 0.08
Ganga basin	Shea and Immerzeel (2016)	-0.29 to -0.76	
Western Himalayan glaciers			
Chhota Shigri glacier	Azam et al. (2014)	-0.52	0.16
Shaune Garang, Gor-Garang, Gara, Siachen	Wang et al. (2019)	-0.83, -0.71, -0.71, -0.24	0.06, 0.06, 0.06, 0.09
Central/eastern Himalayan glaciers			
AX010, Changmekhampu, Yala, Tipra	Wang et al. (2019)	-1.00, -0.66, -0.58, -0.56	0.08, 0.06, 0.05, 0.07
Trambau	Sunako et al. (2019)	-0.90	0.18
Dokriani	Azam and Srivastava (2020)	-1.11	0.24

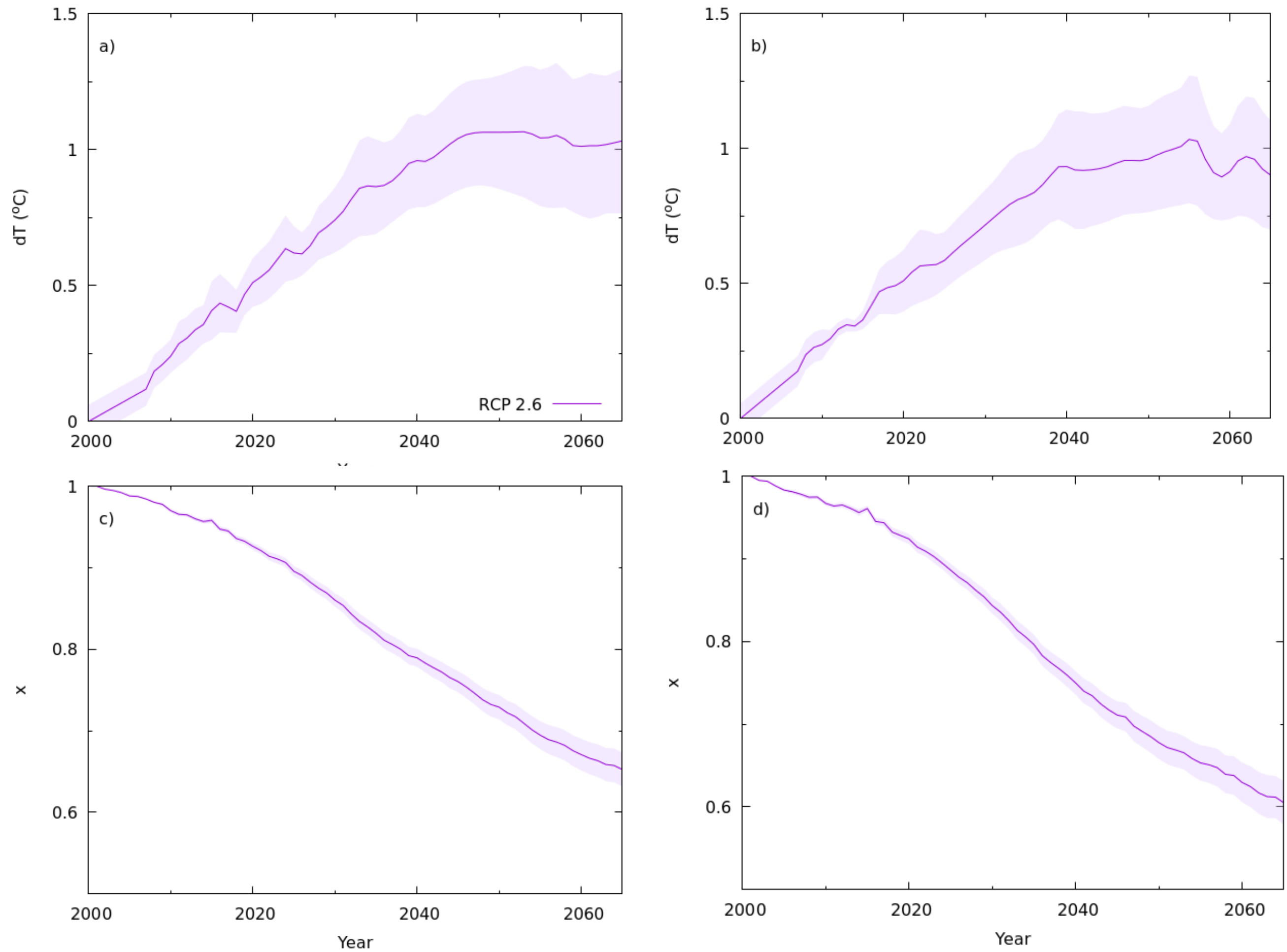

Figure S9. Projected temperature changes over the (a) western, and (b) eastern Himalaya predicted for RCP 2.6 climate scenario (Kraaijenbrink et al., 2017). Kraaijenbrink et al. (2017) provided temperature change data from 2005 onward. Here we extrapolated the data between 2000–2005 using the trend between 2005–2010. Fractional changes in glacier area for (a) Indus, and (b) Ganga basins predicted using RCP 2.6 scenario (Huss and Hock, 2018). In all the four plots, the band is showing the corresponding uncertainties associated with the future projection.